DOI: 10.11844/cjcb.2025.07.0026
中国细胞生物学学报 Chinese Journal of Cell Biology 2025, 47(7): 1740–1749 CSTR: 32200.14.cjcb.2025.07.0026

线粒体形态分析技术研究进展

王大维[1] 王雪苹[1] 刘佳鑫[2] 代旭[3] 曾以德[1] 兰天[1]*
([1]山东中医药大学中医药创新研究院, 济南 250355; [2]山东中医药大学药学院, 济南 250355;
[3]山东中医药大学中医学院, 济南 250355)

摘要 线粒体作为细胞能量代谢与信号调控的核心枢纽, 对其形态变化与功能状态的关联解析是理解细胞生理及病理机制的关键。该文系统性地对线粒体融合–分裂失衡、异常肿胀及分布紊乱等线粒体形态学特征与疾病之间的关联研究进行总结, 聚焦于显微成像技术革新、分子探针开发及智能图像分析方法在线粒体形态学观测与分析研究领域的推动作用。

关键词 线粒体; 线粒体形态分析; 线粒体功能; 显微成像; 分子标记

Advances in Mitochondrial Morphological Analysis Techniques

WANG Dawei[1], WANG Xueping[1], LIU Jiaxin[2], DAI Xu[3], TSENG Yiider[1], LAN Tian[1]*
([1]*Innovation Research Institute of Traditional Chinese Medicine, Shandong University of Traditional Chinese Medicine, Jinan 250355, China*; [2]*College of Pharmaceutical Science, Shandong University of Traditional Chinese Medicine, Jinan 250355, China*;
[3]*College of Traditional Chinese Medicine, Shandong University of Traditional Chinese Medicine, Jinan 250355, China*)

Abstract Mitochondria, serving as the central hub for cellular energy metabolism and signal transduction, are crucial for understanding both cellular physiology and disease mechanisms. A precise elucidation of the relationship between mitochondrial morphological dynamics and functional states is therefore essential. This review systematically synthesizes research on the associations between various mitochondrial morphological features—such as imbalances in fusion-fission dynamics, abnormal swelling, and disorganized spatial distribution—and a range of pathological conditions. Moreover, the review highlights the pivotal role that advances in high-resolution microscopic imaging, the development of innovative molecular probes, and the integration of intelligent image analysis methods have played in enhancing the observation and quantitative analysis of mitochondrial morphology.

Keywords mitochondria; mitochondrial morphology analysis; mitochondrial function; microscopic imaging; molecular labeling

线粒体不仅是细胞能量生成的核心场所, 同时也是细胞内信号转导的关键枢纽, 在生理和众多病理过程中扮演着举足轻重的角色。研究发现, 线粒体功能状态与其形态结构之间存在着紧密且复杂的关联, 其以持续不断的融合与分裂过程对自身的功能状态进行动态调整, 进而满足细胞在不同微环境条件下多样化的功能需求[1]。这一认识为理解线粒体在细胞代谢、程序性死亡及多种疾病中的作用提供了全新的视角。正如QUINTANA-CABRERA[2]所述, 线粒体的形态调控是维持其结构和功能的核心, 也是药物开发中值得关注的潜在的方向。

随着显微成像技术的不断革新以及荧光标记

收稿日期: 2025-02-23 接受日期: 2025-04-17
国家自然科学基金青年基金(批准号: 82305051)、山东省自然科学基金创新发展联合基金(批准号: ZR2022LZY023)和山东省泰山学者特聘专家基金(批准号: tstp20221125)资助的课题
*通信作者。Tel: 15285172656, E-mail: lantian@sdutcm.edu.cn
Received: February 23, 2025 Accepted: April 17, 2025
This work was supported by the National Natural Science Foundation of China (Grant No.82305051), the Shandong Provincial Natural Science Foundation Innovation and Development Joint Funding (Grant No.ZR2022LZY023), and the Taishan Scholar Foundation of Shandong Province (Grant No.tstp20221125)
*Corresponding author. Tel: +86-15285172656, E-mail: lantian@sdutcm.edu.cn

技术的日益成熟, 对线粒体形态变化进行高分辨率、实时性的深入观测已从理论设想转变为实验现实[3]。此外, 机器学习算法与自动化图像分析技术的引入, 更是为线粒体形态学特征的定量分析提供了强有力的技术支撑, 使得对线粒体形态特征的精确描述成为可能[4]。本文旨在系统地梳理和总结近年来线粒体成像技术的最新进展、相关分子探针及荧光蛋白标记的发展以及数据分析的创新应用, 深入探究线粒体形态的动态调控机制及其在疾病发生发展过程中的具体作用机制, 以期为相关领域研究提供全面且深入的参考。

1 线粒体动态重塑与空间分布: 功能调控及疾病病理关联

作为细胞的能量与代谢中心, 线粒体的形态与结构呈现高度的动态。根据细胞的功能需求, 线粒体在细胞内呈现不均匀的动态分布, 同时形成如融合态、碎片态、肿胀等多种形态特征(图1)。而线粒体融合(fussion)与分裂(fission)这两种动态过程则共同维持着线粒体的质量控制, 确保细胞代谢的稳定性。这种空间分布的异质性和形态结构的动态性反映了线粒体自身的功能状态, 并与细胞代谢、凋亡等应激响应以及疾病的发生和发展密切相关。

1.1 线粒体融合: 能量供给与代谢适应

线粒体高度聚合的融合态(fused mitochondria morphology)由线粒体外膜蛋白MFN1/MFN2(mitofusin 1/2)和内膜蛋白OPA1(optic atrophy 1)协同调控而成[5]。当融合过程占主导时, 彼此分离的线粒体进行融合, 从而优化电子传递链功能, 提升氧化磷酸化效率, 提高ATP合成效率, 降低活性氧(reactive oxygen species, ROS)水平[6-7]。具体而言, 在细胞进入G_1/S期转换时, 线粒体呈现网状结构, 膜电位升高, 电子流通性增强, 为细胞分裂提供足够的能量[8]。相类似地, 在低营养环境下, 细胞通过维持线粒体融合态来增加ATP供应, 提高能量利用效率, 以应对能量匮乏, 帮助细胞在代谢压力下生存[9]。再者, 在干细胞的干性维持中, 干细胞通过维持线粒体细长的网络结构, 降低线粒体内ROS水平, 维持自我更新潜能[10]。不仅如此, 融合状态的线粒体还能通过促进氧化磷酸化与增强脂肪酸氧化来支持记忆T细胞的代谢特征, 维持其在体内的长期存活[11]。

1.2 线粒体分裂: 稳态维持与质量控制

当分裂过程占主导时, 线粒体呈现碎片态(frag-

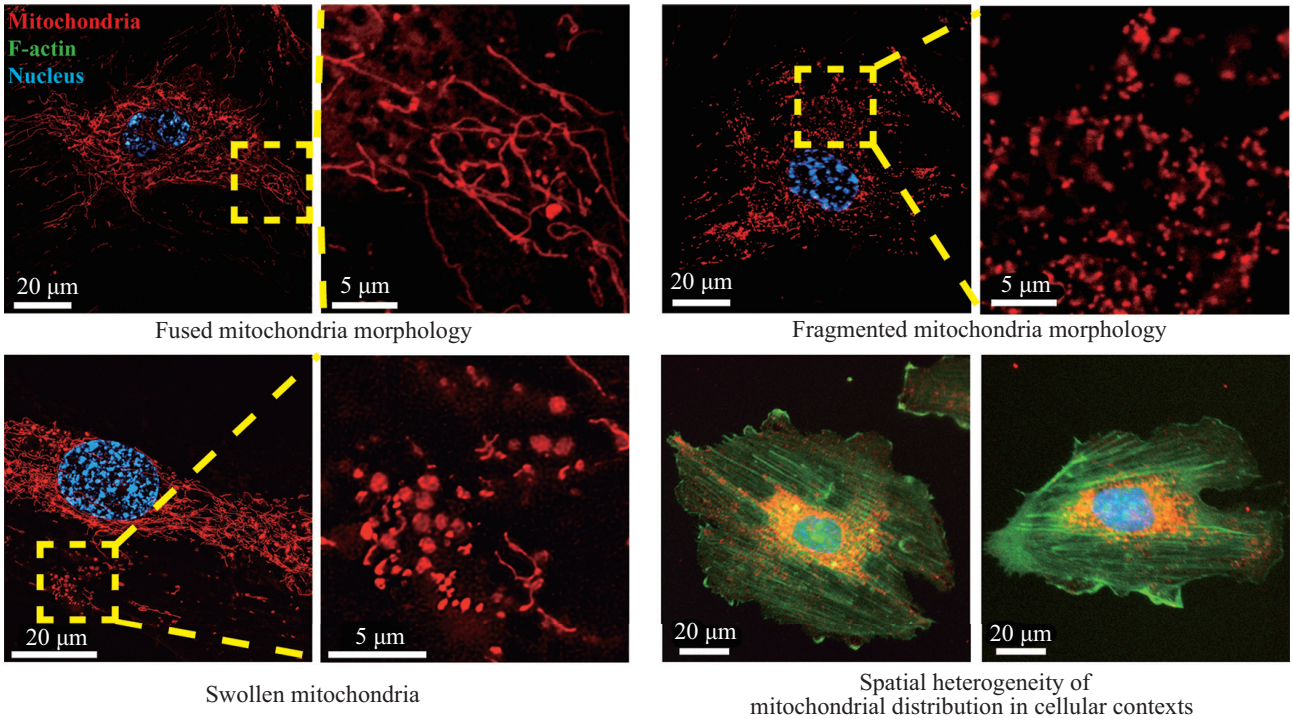

图1 线粒体的不同形态与线粒体在细胞内的不同分布例图

Fig.1 Morphological diversity and spatial distribution patterns of mitochondria: representative imaging

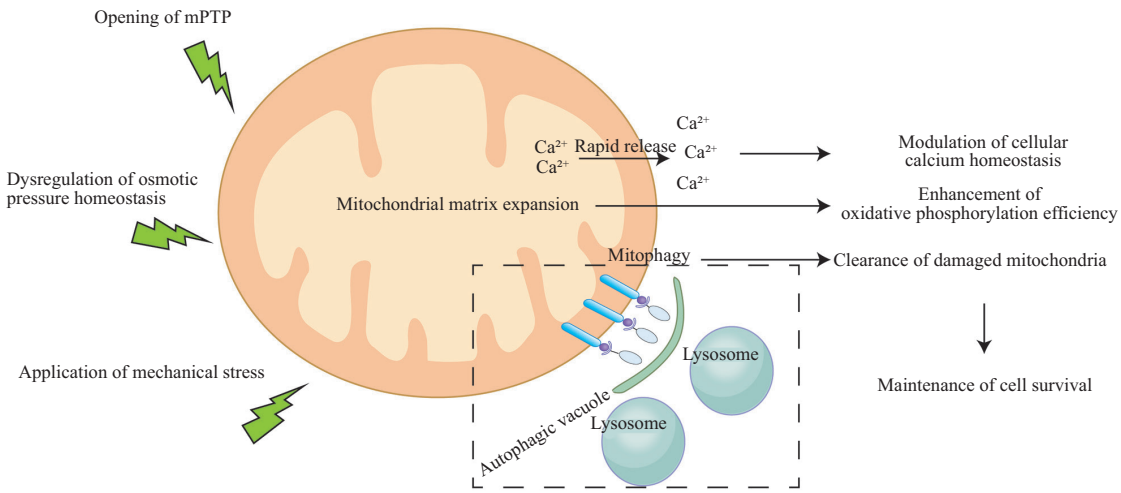

图2 生理性线粒体肿胀与稳态调控示意图

Fig.2 Schematic diagram of physiological mitochondrial swelling and homeostatic regulation

mented mitochondria morphology), 从而降低细胞的能量代谢需求或是支持线粒体进行后续的分裂以及选择性自噬进程。分裂过程由胞质动力相关蛋白Drp1(dynamin-related protein 1)及其线粒体外膜受体(如Fis1、MFF、MiD49/51)协同调控[12]。线粒体分裂态发生在细胞静息期(G_0期)或高营养状态下, 此时ATP需求降低, 线粒体趋向碎片化, 以适应低能耗需求[1,8-9]。分裂过程也是线粒体质量控制的重要环节, 受损的线粒体在分裂过程中进行线粒体自噬(mitophagy), 也就是选择性降解, 同时也为新生线粒体提供模板, 以维持线粒体群体的功能完整性[13]。而在干细胞的定型与分化中, 碎片态的线粒体通常会抑制干细胞的自我更新, 并加速干细胞的定型与分化[14]。除此之外, 在效应T细胞中, 碎片态线粒体通过糖酵解提供大量ATP和中间代谢物(如核苷酸、脂质前体), 支持效应T细胞在感染初期的快速克隆扩增和杀伤功能, 并且更易释放促凋亡因子(如细胞色素C), 使效应T细胞在抗原清除后通过凋亡被淘汰, 防止免疫病理损伤[11]。

1.3 线粒体肿胀: 死亡信号触发与应激适应双刃剑

线粒体肿胀(swollen mitochondria)表现为线粒体基质显著扩张、内膜嵴结构崩解或断裂、外膜完整性部分丧失、整体体积增大并伴随电子密度降低。肿胀过程主要与线粒体通透性转换孔(mitochondrial permeability transition pore, mPTP)的异常开放、渗透压稳态失衡和机械应力驱动相关[15-17], 一般是细胞死亡程序启动的关键信号节点[18]。然而, 在正常生理条件下, 线粒体的适应性肿胀可以作为细胞应激反应的一部分, 在未达到不可逆损伤阈值前启动线粒体自噬, 被溶酶体选择性的自噬降解, 维持细胞存活[19-20]。同时, 肿胀线粒体的mPTP开放过程, 为线粒体提供了Ca^{2+}的快速释放机制, 可调节细胞内钙稳态[16]。另外, 肿胀的线粒体还可以通过其基质的扩张, 增加ADP/ATP交换表面积, 来促进底物水平磷酸化, 以补偿氧化磷酸化效率的下降[17](图2)。

1.4 线粒体分布: 空间动态调控与功能极化

除了形态变化外, 线粒体的分布也与细胞的功能密不可分。线粒体的亚细胞定位受到细胞骨架(如微管、微丝和中间丝)及其相关蛋白的精确调控[21]。在细胞迁移过程中, 线粒体向细胞前缘聚集, 增加局部ATP的含量, 为细胞伪足形成过程中肌动蛋白细胞骨架重塑提供能量[22]。在细胞分裂过程中, 线粒体则通过肌动蛋白与微管的控制, 保证细胞分裂的顺利进行[23-24]。而在神经元树突中线粒体通过细胞骨架锚定, 以稳定的空间隔室存在, 这种局部分布的线粒体可以对神经元突触形态的改变与局部蛋白合成进行供能[25]。此外, 在心肌细胞中, 肌原纤维间的线粒体相对于非肌原纤维间的线粒体, 排列更为紧密, 线粒体嵴密度更高, 可以满足肌原纤维收缩时的高能量需求[26]。

1.5 线粒体形态、分布异常与疾病病理机制的关联

多种疾病与线粒体功能障碍密切相关, 在这些疾病状态下线粒体的形态与分布表型常呈现出特异性的变化。例如, 在神经退行性疾病(如阿尔茨海

默病[27]、肌萎缩侧索硬化症[28]、多发性硬化症[29])、代谢性疾病(如糖尿病[30])以及心血管疾病(如缺血性心脏病[29])中, 疾病相关细胞的线粒体普遍呈现碎片化, 表明其功能受损, 可能导致能量供应不足或细胞凋亡。同时, 在线粒体肌病患者的骨骼肌细胞[31]、非酒精性脂肪性肝炎患者的肝细胞[32]以及心力衰竭患者的心肌细胞[33]中, 线粒体表现出异常肿胀, 提示线粒体功能障碍与代谢稳态失衡。此外, 在多种先天性残疾疾病中(如遗传性痉挛性截瘫、腓骨头肌萎缩症1型等), 相关疾病神经细胞均被发现因线粒体转运功能障碍导致的线粒体分布异常, 引发局部ATP不足与氧化应激, 加速神经元退化[34]。

线粒体的形态变化在恶性肿瘤中尤为突出。当肿瘤细胞的线粒体处于融合态时, 其ATP合成效率显著升高, 从而促进细胞增殖, 帮助肿瘤细胞在恶劣的微环境中维持高速率的生长状态[35]。相反, 肿瘤细胞的线粒体趋于碎片态时, 可以促进肿瘤细胞发生间充质上皮转化, 使其失去细胞–细胞间连接, 细胞前缘丝状伪足的形成能力显著增强, 迁移能力提高, 从而促进肿瘤细胞的侵袭和转移[36], 同时线粒体会向细胞皮层骨架区聚集, 为肿瘤细胞的侵袭提供能量[37]。

线粒体的形态学特征及空间分布不仅决定其能量代谢功能, 还直接影响细胞生理状态。因此, 对线粒体形态的定量分析及其在细胞代谢与疾病发生中的作用研究, 对揭示所处细胞的生命活动具有重要意义。

2 线粒体成像技术与分子工具进展

2.1 显微成像技术的发展推动线粒体研究

线粒体研究的不断深入与显微镜成像技术的革新密不可分(表1)。19世纪中期, 以光学显微镜观察细胞, 首次发现细胞内存在类似颗粒的结构[38]。1890年, ALTMANN[39]通过改良酸性品红染色剂, 观察到这些颗粒几乎在所有细胞类型中存在, 提出这些颗粒可能是独立的细胞器, 并将其称之为“生物粒子”(bioblasts)。1898年, BENDA[40]使用结晶紫染色剂, 发现这些颗粒广泛存在于细胞质中, 有时呈线状(thread-like), 有时呈颗粒状(granule-like), 据此, 他首次提出“线粒体”(mitochondrion)这一名称。20世纪30年代, 商业化荧光显微镜(fluorescence microscope, FM)开始盛行, 为后续使用荧光技术观察线粒体埋下了伏笔[41]。1952年PALADE[42]首次利用透射电子显微镜(transmission electron microscope, TEM)清晰地观察到线粒体的双层膜结构, 并描述了其内膜上具有嵴状褶皱(cristae)的特征。20世纪60~70年代, NOMARSKI[43]改进差分干涉相衬显微镜(differential interference contrast microscopy, DIC), 提升了透明样品的分辨率与立体感, 为线粒体在活细胞内的动态观测提供了技术支持。20世纪80~90年代, 共聚焦显微镜(confocal laser scanning microscopy, CLSM)的广泛应用实现了*x*-*y*轴200 nm, *z*轴500 nm的分辨率, 为线粒体在不同细胞内的空间分布观测提供了新方法[44], 结合荧光探针标记以及三维重构技术, CLSM进一步深化了线粒体在细胞内三维分布[45]、膜运动[46]、电势变化[47]与结构特征[48]等研究。进入21世纪, 超分辨率显微技术的发展[如受激辐射耗尽显微镜(stimulated emission depletion, STED)、随机光学重建显微镜(stochastic optical reconstruction microscopy, STORM)]实现了20~50 nm的观测精度, 进一步揭示了不同疾病细胞中线粒体的精细结构特征及其在细胞凋亡、自噬及细胞器互作中的关键作用[49]。2025年, OUYANG等[50]开发了4Pi-结构照明显微镜(4Pi structured illumination microscopy, 4Pi-SIM), 并将其与活细胞成像技术的结合, 为实时追踪活细胞中线粒体的3D动态行为提供了新的研究手段, 为探讨线粒体的生理功能及其与疾病的关系开启了新的视角。

2.2 线粒体荧光探针与分子标记技术

20世纪初, 德国生物化学家WARBURG[51]通过独创的瓦氏检压技术, 首次实现了线粒体的粗分离, 并从中鉴定出了与细胞呼吸相关的关键酶类(如细胞色素氧化酶)。这一突破性发现直接推动后续科学家开始系统性地解析线粒体膜蛋白(如TOM复合体[52]、ATP合酶[53])的分子结构, 并基于免疫荧光的方法, 采用抗原表位设计特异性抗体标记线粒体外膜(如TOM20蛋白[54])和线粒体内膜(如COXIV蛋白[55]), 实现对线粒体精细结构与功能的可视化研究。20世纪90年代, 随着绿色荧光蛋白(green fluorescent protein, GFP)受到广泛关注并被正式应用于研究[56], 基因工程荧光蛋白被应用到线粒体的形态学研究中。1995年, RIZZUTO团队[57]将GFP与线粒体内膜COX8序列相结合, 这成为活细胞线粒体动态可视化的重要里程碑, 实现了线粒体的特异性定位。

线粒体特异性的荧光探针也为线粒体形态、功

表1 常见显微成像技术对比

Table 1 Comparative analysis of common microscopy imaging techniques

技术 Technique	原理 Principle	分辨率 Resolution	特点 Characteristics	缺点 Limitations
Conventional optical microscope	Based on optical lens imaging principles, magnifies samples through objective and ocular lenses	*x*-*y*: 200 nm	Low cost, user-friendly operation; suitable for macroscopic structural observation of transparent samples	Limited by optical diffraction limit; unable to resolve subcellular structures
FM	Utilizes fluorescent dyes to label target structures; excitation light induces fluorescence, and emitted light is collected via objective lenses	*x*-*y*: 200 nm *z*: 500-700 nm	Rapid imaging; suitable for macroscopic structural analysis with simple operation	Limited by optical diffraction limit; unable to resolve subcellular structures
DIC	Employs polarized light and differential interference to convert sample thickness/refractive index variations into 3D relief-like contrast	*x*-*y*: 200 nm	High stereoscopy imaging; rich structural details; ideal for transparent samples	Incompatible with plastic culture dishes; imaging artifacts may arise from material interference
CLSM	Laser-based point scanning combined with pinhole detection to eliminate out-of-focus signals, enabling optical sectioning and 3D reconstruction	*x*-*y*: 200 nm *z*: 500 nm	High resolution, non-destructive imaging; suitable for live-cell imaging; multicolor labeling, and 3D analysis	Complex operation; high cost; photobleaching may occur
STORM	Achieves super-resolution via single-molecule localization by stochastically activating fluorescent probes and reconstructing images	*x*-*y*: 20-50 nm *z*: 50-100 nm	Ultrahigh resolution; compatible with live- and fixed-cell imaging	Requires specialized fluorescent probes; prolonged imaging time
STED	Overcomes diffraction limit by suppressing peripheral fluorescence emission using depletion beams	*x*-*y*: 20-50 nm *z*: 50-100 nm	Ultrahigh resolution; compatible with live- and fixed-cell imaging	Demands specialized probes; photobleaching may occur
SIM	Enhances resolution via structured illumination patterns and computational reconstruction algorithms	*x*-*y*: 100 nm *z*: 200-300 nm	Super-resolution imaging; applicable to live- and fixed-cell systems	Requires complex image processing algorithms; prolonged imaging time
TEM	Electron beam transmits through ultrathin sections, magnified by electromagnetic lenses to reveal ultrastructural details	*x*-*y*: 0.1-1 nm	Exceptional resolution for subcellular structures and biomolecules	Specialized sample processing required; technically complex
Cryo-electron microscopy	Preserves native-state samples at cryogenic temperatures for electron beam imaging	*x*-*y*: 0.1 nm	Ideal for temperature-sensitive specimens (e.g., proteins, biological sections)	Specialized sample processing required; technically complex

能的研究创造了条件(表2)。1981年, JOHNSON等[58]基于线粒体内外膜的电位差(ΔΨm)开发了染料罗丹明123(Rhodamine 123), 实现了线粒体膜电位的实时检测, 揭示了线粒体在能量代谢中的动态极化特征。随后, 可以反应线粒体膜电位的罗丹明类(TMRE、TMRM)、JC-1类等染料一步步被开发出来。基于罗丹明染料衍生物发展的MitoTracker系列探针通过共价结合线粒体内膜蛋白, 克服了传统染剂在固定和渗透处理后丧失荧光的局限性, 实现了线粒体形态的长时程稳定标记[59]。21世纪以来, 光转换荧光蛋白与超分辨率兼容探针的研发极大提升了成像精度。2014年, SHENG的团队[60]使用Mito-Killer Red探针, 利用光毒性特异性诱导线粒体损伤, 为研究线粒体自噬与形态修复机制提供了可控工具。

3 图像分析方法及应用

显微成像技术与分子标记技术的发展拓展了线粒体的捕捉精度和观测的时空范围。影像数据

表2 常见线粒体标记荧光探针特性对比

Table 2 Comparative analysis of common mitochondria-targeting fluorescent probes

荧光探针类型 Fluorescent probe type	标记原理及特点 Labeling principle and characteristics	细胞类型 Compatible cell types	常用成像技术 Applicable imaging techniques
Rhodamine 123	Cationic and lipophilic fluorescent probe. Penetrates cell membranes and accumulates in the matrix via the mitochondrial inner membrane potential gradient (ΔΨm). Fluorescence intensity correlates with ΔΨm	Live cells	FM, CLSM, SIM
TMRM		Live cells	FM, CLSM, SIM, STED
TMRE		Live cells	FM, CLSM, SIM
MitoTracker	ΔΨm-dependent accumulation in active mitochondria. Specific variants (e.g., MitoTracker Red CMXRos) contain chloromethyl groups that covalently bind to mitochondrial proteins post-entry, enabling signal retention after fixation	Live cells Fixed cells	FM, CLSM, SIM, STED, STORM
MitoLite	Cationic dye selectively accumulating in mitochondria via ΔΨm	Live cells Fixed cells	FM, CLSM, SIM, STED
PKMito		Live cells Fixed cells	FM, CLSM, SIM, STED
MitoBright		Live cells	FM, CLSM, SIM
BBcellProbe M		Live cells	FM, CLSM, SIM
HBmito		Live cells	FM, CLSM, SIM, STED
MitoSOX	Modified dihydroethidium-based probe with positive charge for mitochondrial-specific uptake. Generates fluorescence upon reaction with superoxide anions to detect mitochondrial ROS	Live cells	FM, CLSM, SIM, STED
CellLight	Fluorescent protein-based labeling technology. Delivers fluorescent proteins (e.g., GFP/RFP) fused with mitochondrial localization signals into cells, independent of ΔΨm	Live cells	FM, CLSM, SIM

的爆炸式扩展导致“如何实现线粒体的定量分析”成为关键问题。近年来, 随着图像分析技术的发展, 高通量的线粒体分析方法与机器学习的分析方法应运而生, 成为精准研究线粒体形态的有力工具, 也为相关疾病的机制探索和药物筛选开辟了新途径。

3.1 线粒体形态分析的常用特征参数

定量分析线粒体时, 特征参数的选择十分重要。常用的参数包括: 长度、面积、圆度、分支数、网络连通性等(表3)。它们均能够在一定程度上反映线粒体处于融合/分裂的状态。例如: 史雪敬等[61]对线粒体的圆度、面积等参数进行分析, 反映线粒体的融合状态, 并由此筛选出了人参/三七中对心肌起到主要保护作用的物质。JUN等[62]用线粒体长度反映线粒体的网络状态及功能, 并以此探究丙型肝炎病毒所诱导的线粒体功能障碍在人参皂苷Rg3干预下的恢复作用。OUELLET等[63]通过线粒体长度、面积、分支点、网络连通性等参数对线粒体网络结构进行评估, 通过影像学识别应力诱导的线粒体连通性和内膜结构的改变。

3.2 图像分割算法

在基于线粒体的显微图像形态特征提取研究中, 图像分割是量化分析的关键预处理步骤, 其质量直接影响到后续对线粒体长度、圆度、分支数、网络连通性等形态计量参数的准确计算(图3)。传统分割算法主要依据线粒体的灰度特征、几何形态和拓扑结构特点进行设计, 可分为四大类方法: 阈值分割(利用线粒体与背景的灰度差异进行分割)、边缘检测(通过Canny等算子检测线粒体边界梯度突变进行分割)、区域生长(以种子点为中心, 通过像素相似性准则迭代合并相邻像素进行分割)及活动轮廓模型(采用参数化曲线或几何流拟合线粒体边界进行分割)。在线粒体的形态学分析中, 常常根据线粒体亚细胞结构的灰度分布、纹理特征和拓扑特性, 通过单一或组合的分割策略对线粒体轮廓进行精准分割, 从而为后续的长度、圆度、分支数、网络连通性等形态计量学分析奠定基础。

3.3 常用的形态分析工具集

随着技术的进步, 自动化图像工具集在形态分

表3 常用线粒体形态分析特征参数

Table 3 Key parameters for quantitative analysis of mitochondrial morphology

特征参数 Parameter	定义 Definition	计算方式 Calculation method	意义 Biological significance
Length	The longest axial distance of mitochondria	Calculated as the major axis length of the minimum bounding rectangle fitted to the mitochondrial contour	Elongated mitochondria are typically associated with active energy metabolism (fusion-dominant state), while shortened forms may indicate fission defects or functional impairment
Width	The diameter along the minor axis of mitochondria	Calculated as the minor axis length of the minimum bounding rectangle	Width variations may reflect rearrangements of inner membrane cristae or matrix swelling
Area	Two-dimensional projected coverage of mitochondria	Direct measurement of pixel occupancy	Increased area suggests mitochondrial fusion or matrix expansion, whereas reduced area correlates with fission events or autophagic clearance
Circularity	Degree to which mitochondrial shape approximates a perfect circle	$4\pi \times \frac{\text{Area}}{(\text{Perimeter})^2}$	Values approaching 1 indicate spherical morphology (often linked to quiescent/damaged states, e.g., swelling), while lower values reflect rod-shaped or tubular structures (typically active functional states)
Branch number	Number of branches in the mitochondrial network	Direct count of terminal and internal branches	Increased branching implies network complexity, potentially driven by elevated energy demands; reduced branching may signify network fragmentation or functional decline
Network connectivity	Interconnection degree between nodes (branch points) in the mitochondrial network	$\frac{\text{Branch points number}}{\text{Branch number}}$	High connectivity indicates efficient energy distribution networks, while low connectivity suggests network disintegration or functional compartmentalization
Spatial distribution	Spatial organization pattern of mitochondria within the cellular context	Quantified by region-specific mitochondrial density (e.g., perinuclear zones vs. cortical zones) or proximity to organelles (e.g., endoplasmic reticulum)	Mitochondria preferentially localize to high energy-demand regions (e.g., synaptic terminals). Abnormal distribution may reflect bioenergetic imbalance or organelle interaction defects

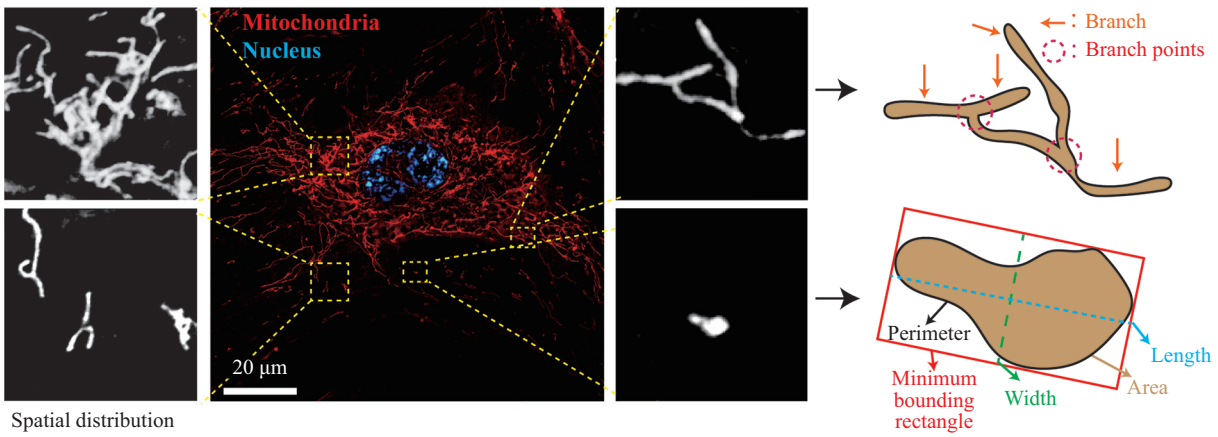

图3 常用线粒体形态分析特征参数示意图

Fig.3 Illustration of key parameters in mitochondrial morphological analysis

析方面取得了显著进展。这些技术能够精确、快速地处理和分析大量的线粒体图像，极大地提升了研究效率。

例如，ROHANI等[64]开发的Mito Hacker工具集，能有效提取单细胞水平的线粒体网络数据。它通过自动分离和去除背景噪声，实现高通量的线粒体形态分析，为大规模数据的生成和分析提供了基础。LEFEBVRE等[35]开发的Mitometer工具集，可用在活

细胞时序动态图像中快速、准确地分割和跟踪线粒体。该工具通过形状保留与背景去除等方法, 能够独立区分线粒体, 实现在时间尺度上对线粒体高效动态监测。FISCHER等[65]开发的MitoSegNet工具集是一个基于预训练的深度学习分割模型, 能够高效地量化线粒体形态。该模型给研究人员提供了便捷的深度学习应用平台, 极大程度地推动了线粒体形态学研究的标准化和自动化。此外, CHU等[4]对多种图像分析工具和机器学习技术在不同癌细胞系中线粒体形态表型的应用进行总结, 强调了多参数分析在癌症研究中的潜力。这些方法不仅能够量化线粒体形态的动态变化, 还能够揭示线粒体功能与疾病之间的潜在联系。

4 结论与展望

综上所述, 线粒体作为细胞能量代谢、信号转导及程序性死亡的核心调控中心, 其结构和功能的深入研究对于理解细胞生理过程和疾病机制具有重要意义。线粒体研究的重大进展主要依赖于显微成像技术与分子标记技术的协同创新, 从光学显微镜到透射电镜、共聚焦显微镜, 再到超分辨率显微镜, 显微成像技术的不断进步使研究者能够更清晰地观察线粒体的精细结构, 并且分子标记技术也从传统的免疫荧光发展到光转换荧光蛋白和超分辨率探针, 实现了对线粒体动态过程的高精度示踪。与此同时, 基于传统算法与现代深度学习技术的自动化图像分割与定量分析工具的发展, 为大规模、精准的线粒体形态学特征提取提供了有力支撑。

随着技术的发展, 线粒体的研究也正在向长时程、高精度、多维度方向迈进。在荧光探针方面, 研究者们通过对传统染料的结构优化和新型探针的开发, 成功设计出越来越多低光毒性、多荧光标记、高光稳定性的分子探针, 如Mulberrin-Cy3[66]、Nile Blue Probes[67]等。此外, “多功能”荧光探针的兴起, 如ATP荧光探针[68]、Ca^{2+}荧光探针[69]等, 使得单次实验即可同时检测多种生理数据。在显微成像技术方面, 高分辨率、高扫描速度为线粒体动态研究提供了前所未有的时空分辨率, 如MINFLUX超分辨技术可将3D分辨率提升至1~3 nm[70], 而sCMOS成像技术可以将采集速度提升至250 000帧/秒等。与此同时, 智能图像分析算法的发展也正在突破生物复杂系统的解析瓶颈。如HANDLEY等[71]开发的AutoMitoNetwork可以基于线粒体自发荧光成像来对线粒体进行形态特征分析, MIDTVEDT团队[72]开发的深度学习算法LodeSTAR大幅减少了训练数据量的需求, 并在亚细胞器层面实现了更高的识别精度。未来, 多模态成像技术的融合应用, 如超分辨光学显微与电子显微技术联合使用[73], 将进一步推动跨尺度、跨平台的线粒体结构与功能的研究, 为解析线粒体动力学、代谢调控与病理机制提供更强大的工具。

参考文献 (References)

[1] CHEN W, ZHAO H, LI Y. Mitochondrial dynamics in health and disease: mechanisms and potential targets [J]. Signal Transduct Target Ther, 2023, 8(1): 333.

[2] QUINTANA-CABRERA R, SCORRANO L. Determinants and outcomes of mitochondrial dynamics [J]. Mol Cell, 2023, 83(6): 857-76.

[3] JAKOBS S. High resolution imaging of live mitochondria [J]. Biochim Biophys Acta, 2006, 1763(5/6): 561-75.

[4] CHU C H, TSENG W W, HSU C M, et al. Image analysis of the mitochondrial network morphology with applications in cancer research [J]. Front Phys, 2022, 10: 855775.

[5] ADEBAYO M, SINGH S, SINGH A P, et al. Mitochondrial fusion and fission: the fine-tune balance for cellular homeostasis [J]. Faseb J, 2021, 35(6): e21620.

[6] ASHRAF R, KUMAR S. Mfn2-mediated mitochondrial fusion promotes autophagy and suppresses ovarian cancer progression by reducing ROS through AMPK/mTOR/ERK signaling [J]. Cell Mol Life Sci, 2022, 79(11): 573.

[7] CHAKRABARTY R P, CHANDEL N S. Mitochondria as signaling organelles control mammalian stem cell fate [J]. Cell Stem Cell, 2021, 28(3): 394-408.

[8] MITRA K, WUNDER C, ROYSAM B, et al. A hyperfused mitochondrial state achieved at G_1-S regulates cyclin E buildup and entry into S phase [J]. Proc Natl Acad Sci USA, 2009, 106(29): 11960-5.

[9] MOLINA A J, WIKSTROM J D, STILES L, et al. Mitochondrial networking protects beta-cells from nutrient-induced apoptosis [J]. Diabetes, 2009, 58(10): 2303-15.

[10] BAKER N, WADE S, TRIOLO M, et al. The mitochondrial protein OPA1 regulates the quiescent state of adult muscle stem cells [J]. Cell Stem Cell, 2022, 29(9): 1315-32,e9.

[11] BUCK M D, O'SULLIVAN D, KLEIN GELTINK R I, et al. Mitochondrial dynamics controls T cell fate through metabolic programming [J]. Cell, 2016, 166(1): 63-76.

[12] TÁBARA L C, SEGAWA M, PRUDENT J. Molecular mechanisms of mitochondrial dynamics [J]. Nat Rev Mol Cell Biol, 2025, 26(2): 123-46.

[13] KLEELE T, REY T, WINTER J, et al. Distinct fission signatures predict mitochondrial degradation or biogenesis [J]. Nature, 2021, 593(7859): 435-9.

[14] SOMMERS O, TOMSINE R A, KHACHO M. Mitochondrial dynamics drive muscle stem cell progression from quiescence to myogenic differentiation [J]. Cells, 2024, 13(21): 1773.

[15] BERNARDI P, DI LISA F. The mitochondrial permeability transition pore: molecular nature and role as a target in cardioprotection [J]. J Mol Cell Cardiol, 2015, 78: 100-6.
[16] BERNARDI P, GERLE C, HALESTRAP A P, et al. Identity, structure, and function of the mitochondrial permeability transition pore: controversies, consensus, recent advances, and future directions [J]. Cell Death Differ, 2023, 30(8): 1869-85.
[17] KHMELINSKII I, MAKAROV V. Reversible and irreversible mitochondrial swelling *in vitro* [J]. Biophys Chem, 2021, 278: 106668.
[18] GODOY J A, RIOS J A, PICÓN-PAGÈS P, et al. Mitostasis, calcium and free radicals in health, aging and neurodegeneration [J]. Biomolecules, 2021, 11(7): 1012.
[19] LEMASTERS J J. Selective mitochondrial autophagy, or mitophagy, as a targeted defense against oxidative stress, mitochondrial dysfunction, and aging [J]. Rejuvenation Res, 2005, 8(1): 3-5.
[20] LEE C, NAM J S, LEE C G, et al. Analysing the mechanism of mitochondrial oxidation-induced cell death using a multifunctional iridium(III) photosensitiser [J]. Nat Commun, 2021, 12(1): 26.
[21] SHAH M, CHACKO L A, JOSEPH J P, et al. Mitochondrial dynamics, positioning and function mediated by cytoskeletal interactions [J]. Cell Mol Life Sci, 2021, 78(8): 3969-86.
[22] CUNNIFF B, MCKENZIE A J, HEINTZ N H, et al. AMPK activity regulates trafficking of mitochondria to the leading edge during cell migration and matrix invasion [J]. Mol Biol Cell, 2016, 27(17): 2662-74.
[23] ROHN J L, PATEL J V, NEUMANN B, et al. Myo19 ensures symmetric partitioning of mitochondria and coupling of mitochondrial segregation to cell division [J]. Curr Biol, 2014, 24(21): 2598-605.
[24] CHUNG J Y, STEEN J A, SCHWARZ T L. Phosphorylation-induced motor shedding is required at mitosis for proper distribution and passive inheritance of mitochondria [J]. Cell Rep, 2016, 16(8): 2142-55.
[25] RANGARAJU V, LAUTERBACH M, SCHUMAN E M. Spatially stable mitochondrial compartments fuel local translation during plasticity [J]. Cell, 2019, 176(1/2): 73-84,e15.
[26] ADAMS R A, LIU Z, HSIEH C, et al. Structural analysis of mitochondria in cardiomyocytes: insights into bioenergetics and membrane remodeling [J]. Curr Issues Mol Biol, 2023, 45(7): 6097-115.
[27] SHAH S I, PAINE J G, PEREZ C, et al. Mitochondrial fragmentation and network architecture in degenerative diseases [J]. PLoS One, 2019, 14(9): e0223014.
[28] REY F, OTTOLENGHI S, ZUCCOTTI G V, et al. Mitochondrial dysfunctions in neurodegenerative diseases: role in disease pathogenesis, strategies for analysis and therapeutic prospects [J]. Neural Regen Res, 2022, 17(4): 754-8.
[29] KATHIRESAN D S, BALASUBRAMANI R, MARUDHACHALAM K, et al. Role of mitochondrial dysfunctions in neurodegenerative disorders: advances in mitochondrial biology [J]. Mol Neurobiol, 2024: 1-29.
[30] ZHENG L, RAO Z, GUO Y, et al. High-intensity interval training restores glycolipid metabolism and mitochondrial function in skeletal muscle of mice with type 2 diabetes [J]. Front Endocrinol, 2020, 11: 561.
[31] VINCENT A E, NG Y S, WHITE K, et al. The spectrum of mitochondrial ultrastructural defects in mitochondrial myopathy [J]. Sci Rep, 2016, 6: 30610.
[32] AMORIM J A, COPPOTELLI G, ROLO A P, et al. Mitochondrial and metabolic dysfunction in ageing and age-related diseases [J]. Nat Rev Endocrinol, 2022, 18(4): 243-58.
[33] CHAANINE A H, JOYCE L D, STULAK J M, et al. Mitochondrial morphology, dynamics, and function in human pressure overload or ischemic heart disease with preserved or reduced ejection fraction [J]. Circ Heart Fail, 2019, 12(2): e005131.
[34] KUMAR SHARMA R, CHAFIK A, BERTOLIN G. Mitochondrial transport, partitioning, and quality control at the heart of cell proliferation and fate acquisition [J]. Am J Physiol Cell Physiol, 2022, 322(2): C311-C25.
[35] LEFEBVRE A, MA D, KESSENBROCK K, et al. Automated segmentation and tracking of mitochondria in live-cell time-lapse images [J]. Nat Methods, 2021, 18(9): 1091-102.
[36] HAN L, ZHANG C, WANG D, et al. Retrograde regulation of mitochondrial fission and epithelial to mesenchymal transition in hepatocellular carcinoma by GCN5L1 [J]. Oncogene, 2023, 42(13): 1024-37.
[37] BERTOLINI I, KEENEY F, ALTIERI D C. Protocol for assessing real-time changes in mitochondrial morphology, fission and fusion events in live cells using confocal microscopy [J]. STAR Protoc, 2021, 2(3): 100767.
[38] GLANCY B, KANE D A, KAVAZIS A N, et al. Mitochondrial lactate metabolism: history and implications for exercise and disease [J]. J Physiol, 2021, 599(3): 863-88.
[39] ALTMANN R. Die Elementarorganismen und ihre Beziehungen zu den Zellen [M]. Berlin: De Gruyter, 1894.
[40] BENDA C. Ueber die spermatogenese der vertebraten und höherer evertebraten, II. Theil: die histiogenese der spermien [J]. Arch Anat Physiol, 1898, 73: 393-8.
[41] LAKOWICZ J R. Principles of fluorescence spectroscopy [M]. Boston: Springer, 2006.
[42] PALADE G E. A study of fixation for electron microscopy [J]. J Exp Med, 1952, 95(3): 285-98.
[43] NOMARSKI G. Microinterféromètre différentiel à ondes polarisées [J]. J Phys Rad, 1955, 16: 9S-13S.
[44] WHITE J G, AMOS W B, FORDHAM M. An evaluation of confocal versus conventional imaging of biological structures by fluorescence light microscopy [J]. J Cell Biol, 1987, 105(1): 41-8.
[45] AHMADIAN S, LINDSEY P J, SMEETS H J M, et al. Spinning disk confocal microscopy for optimized and quantified live Imaging of 3D mitochondrial network [J]. Int J Mol Sci, 2024, 25(9): 15.
[46] KONING A J, LUM P Y, WILLIAMS J M, et al. DiOC6 staining reveals organelle structure and dynamics in living yeast cells [J]. Cell Motil Cytoskeleton, 1993, 25(2): 111-28.
[47] SUGRUE M M, WANG Y, RIDEOUT H J, et al. Reduced mitochondrial membrane potential and altered responsiveness of a mitochondrial membrane megachannel in p53-induced senescence [J]. Biochem Biophys Res Commun, 1999, 261(1): 123-30.
[48] MARCHANT J S, RAMOS V, PARKER I. Structural and functional relationships between Ca^{2+} puffs and mitochondria in xenopus oocytes [J]. Am J Physiol Cell Physiol, 2002, 282(6): C1374-

86.

[49] REN W, GE X, LI M, et al. Author correction: visualization of cristae and mtDNA interactions via STED nanoscopy using a low saturation power probe [J]. Light Sci Appl, 2024, 13(1): 235.

[50] OUYANG Z, WANG Q, LI X, et al. Elucidating subcellular architecture and dynamics at isotropic 100-nm resolution with 4Pi-SIM [J]. Nat Methods, 2025, 22(2): 335-47.

[51] WARBURG O. Über Eisen, den sauerstoff-übertragenden bestandteil des atmungsferments [J]. Berichte Der Deutschen Chemischen Gesellschaft, 1925, 58(6): 1001-11.

[52] MOCZKO M, DIETMEIER K, SÖLLNER T, et al. Identification of the mitochondrial receptor complex in *Saccharomyces cerevisiae* [J]. FEBS Lett, 1992, 310(3): 265-8.

[53] ABRAHAMS J P, LESLIE A G, LUTTER R, et al. Structure at 2.8 A resolution of F1-ATPase from bovine heart mitochondria [J]. Nature, 1994, 370(6491): 621-8.

[54] SUN C, LI P, ZHANG G, et al. Investigation of mitochondrial homeostasis changes in lens epithelium of high-myopic cataract [J]. Curr Eye Res, 2024, 49(2): 158-67.

[55] PACKIRISWAMY N, COULSON K F, HOLCOMBE S J, et al. Oxidative stress-induced mitochondrial dysfunction in a normal colon epithelial cell line [J]. World J Gastroenterol, 2017, 23(19): 3427-39.

[56] CHALFIE M, TU Y, EUSKIRCHEN G, et al. Green fluorescent protein as a marker for gene expression [J]. Science, 1994, 263(5148): 802-5.

[57] RIZZUTO R, BRINI M, PIZZO P, et al. Chimeric green fluorescent protein as a tool for visualizing subcellular organelles in living cells [J]. Curr Biol, 1995, 5(6): 635-42.

[58] JOHNSON L V, WALSH M L, BOCKUS B J, et al. Monitoring of relative mitochondrial membrane potential in living cells by fluorescence microscopy [J]. J Cell Biol, 1981, 88(3): 526-35.

[59] POOT M, ZHANG Y Z, KRÄMER J A, et al. Analysis of mitochondrial morphology and function with novel fixable fluorescent stains [J]. J Histochem Cytochem, 1996, 44(12): 1363-72.

[60] ERTÜRK A, WANG Y, SHENG M. Local pruning of dendrites and spines by caspase-3-dependent and proteasome-limited mechanisms [J]. J Neurosci, 2014, 34(5): 1672-88.

[61] 史雪敬, 陈彦羽, 蔡思怡, 等. 基于线粒体形态特征与UPLC-Triple-TOF-MS整合分析的人参/三七心肌保护物质辨析研究 [J]. 中国中药杂志(SHI X, CEHN Y, CAI S, et al. Identification of cardioprotective substances in Panax ginseng/P. notoginseng based on mitochondrial morphological characteristics and UPLC-Triple-TOF-MS [J]. China J Chin Mater Medica), 2024, 49(10): 2766-75.

[62] KIM S J, JANG J Y, KIM E J, et al. Ginsenoside Rg3 restores hepatitis C virus-induced aberrant mitochondrial dynamics and inhibits virus propagation [J]. Hepatology, 2017, 66(3): 758-71.

[63] OUELLET M, GUILLEBAUD G, GERVAIS V, et al. A novel algorithm identifies stress-induced alterations in mitochondrial connectivity and inner membrane structure from confocal images [J]. PLoS Comput Biol, 2017, 13(6): e1005612.

[64] ROHANI A, KASHATUS J A, SESSIONS D T, et al. Mito hacker: a set of tools to enable high-throughput analysis of mitochondrial network morphology [J]. Sci Rep, 2020, 10(1): 18941.

[65] FISCHER C A, BESORA-CASALS L, ROLLAND S G, et al. MitoSegNet: easy-to-use deep learning segmentation for analyzing mitochondrial morphology [J]. iScience, 2020, 23(10): 101601.

[66] YUAN G, LUO Y, QIAN P, et al. Mitochondrial labeling with mulberrin-cy3: a new fluorescent probe for live cell visualization [J]. Biosensors, 2024, 14(9): 428.

[67] LI Y, BAI X, YANG D. Development and aplication of cationic nile blue probes in live-cell super-resolution imaging and specific targeting to mitochondria [J]. ACS Cent Sci, 2024, 10(6): 1221-30.

[68] WANG L, YUAN L, ZENG X, et al. A multisite-binding switchable fluorescent probe for monitoring mitochondrial ATP level fluctuation in live cells [J]. Angew Chem Int Ed Engl, 2016, 55(5): 1773-6.

[69] WERLEY C A, BOCCARDO S, RIGAMONTI A, et al. Multiplexed optical sensors in arrayed islands of cells for multimodal recordings of cellular physiology [J]. Nat Commun, 2020, 11(1): 3881.

[70] SCHMIDT R, WEIHS T, WURM C A, et al. MINFLUX nanometer-scale 3D imaging and microsecond-range tracking on a common fluorescence microscope [J]. Nat Commun, 2021, 12(1): 1478.

[71] HANDLEY S, ANWER A G, KNAB A, et al. AutoMitoNetwork: software for analyzing mitochondrial networks in autofluorescence images to enable label-free cell classification [J]. Cytometry A, 2024, 105(9): 688-703.

[72] MIDTVEDT B, PINEDA J, SKÄRBERG F, et al. Single-shot self-supervised object detection in microscopy [J]. Nat Commun, 2022, 13(1): 7492.

[73] CHEN J, STEPHAN T, GAEDKE F, et al. An aldehyde-cross-linking mitochondrial probe for STED imaging in fixed cells [J]. Proc Natl Acad Sci, 2024, 121(19): e2317703121.